Acid-sensing ion channels emerged over 600 Mya and are conserved throughout the deuterostomes

Timothy Lynagh[a,1], Yana Mikhaleva[b], Janne M. Colding[a], Joel C. Glover[b,c], and Stephan A. Pless[a]

[a]Department of Drug Design and Pharmacology, Center for Biopharmaceuticals, University of Copenhagen, 2100 Copenhagen, Denmark; [b]Sars International Centre for Marine Molecular Biology, University of Bergen, 5006 Bergen, Norway; and [c]Department of Molecular Medicine, University of Oslo, 0372 Oslo, Norway

Edited by Richard W. Aldrich, The University of Texas at Austin, Austin, TX, and approved June 28, 2018 (received for review April 17, 2018)

Acid-sensing ion channels (ASICs) are proton-gated ion channels broadly expressed in the vertebrate nervous system, converting decreased extracellular pH into excitatory sodium current. ASICs were previously thought to be a vertebrate-specific branch of the DEG/ENaC family, a broadly conserved but functionally diverse family of channels. Here, we provide phylogenetic and experimental evidence that ASICs are conserved throughout deuterostome animals, showing that ASICs evolved over 600 million years ago. We also provide evidence of ASIC expression in the central nervous system of the tunicate, *Oikopleura dioica*. Furthermore, by comparing broadly related ASICs, we identify key molecular determinants of proton sensitivity and establish that proton sensitivity of the ASIC4 isoform was lost in the mammalian lineage. Taken together, these results suggest that contributions of ASICs to neuronal function may also be conserved broadly in numerous animal phyla.

ASIC evolution | ligand recognition | invertebrate | nervous system | proton sensing

Neurons are set apart from other cells by their rapid conduction and exchange of information. This is in large part due to ligand-gated ion channels, membrane-bound receptors that convert chemical information, such as neurotransmitter release, into electrical current (1). Not surprisingly, the evolution of nervous systems is intricately linked to the emergence and expansion of ligand-gated ion channels in the genome (2). For example, certain neurotransmitter receptor families seem to have expanded uniquely in those basal animals with nervous systems (3), and these include the glutamate receptors typically associated with fast synaptic transmission and plasticity (4, 5).

It has recently emerged that protons act as neurotransmitters at certain glutamatergic synapses in the mammalian brain, where excitatory current through acid-sensing ion channels (ASICs) is required for synaptic plasticity (6, 7). This follows from several experiments implicating hippocampal and amygdala ASICs in learning and memory, fear, and depression (8). Members of the ASIC family have been cloned from simpler chordates, including the tunicate *Ciona intestinalis* and the jawless fish *Lampetra fluviatilis*, but these did not respond to protons (9, 10). This raises the possibility that proton sensitivity of ASICs emerged within the jawed vertebrates, well after this lineage had split from other, simpler deuterostome animals (9, 10). However, ASICs are widely distributed in the vertebrate nervous system and contribute to behaviors that are conserved across most animals, including nociception, chemosensation, and mechanosensation (11, 12). Furthermore, ASICs derive from the degenerin/epithelial Na^+ channel (DEG/ENaC) family, genes of which are conserved throughout all major animal lineages (3), and some of which are expressed in invertebrate postsynaptic membranes (13). These facts are difficult to reconcile with ASICs being limited to the jawed vertebrates.

DEG/ENaC subunits form trimeric channels of diverse function. Examples include mechanically gated channels in roundworms (14), peptide-gated channels in snails and hydra (15, 16), and constitutively active ENaCs in vertebrates (17). It seems plausible that proton-gated channels could also contribute to physiology in more diverse animal lineages, and that we should therefore find ASICs in nonvertebrate genomes. However, previous studies suggest that ASICs are not readily identifiable through sequence analyses alone (9). This is likely due to our poor understanding of the molecular determinants of proton sensitivity, notwithstanding the finding that the mutation of several protonatable side chains in the extracellular domain decreases proton sensitivity of ASICs (18–22).

Here, we sought to illuminate the evolutionary emergence of ASICs and the molecular basis of proton sensing. Combining recent genetic data with molecular phylogenetics and electrophysiological recordings, we identified functional ASICs from a more representative sample of animals than previously possible. Through various mutagenesis experiments, we established determinants of proton-gated currents that underlie proton sensitivity throughout the ASIC family. Our results show that ASICs evolved much earlier than previously thought, suggest that proton-gated currents may contribute to neuronal signaling throughout deuterostome animals, and point toward a mechanism of proton sensing involving several parts of the channel.

Results

Proton-Gated ASICs Are Conserved Throughout the Deuterostomes. The phylum Chordata includes vertebrates, tunicates (sister taxon to vertebrates), and cephalochordates (23). Chordates, together with echinoderms and hemichordates, comprise the deuterostomes, which are distinct from protostomes (e.g., mollusks, arthropods, and roundworms) and from the xenacoelomorphs (24). Together,

Significance

The conversion of extracellular chemical signals into electrical current across the cell membrane is a defining characteristic of the nervous system. This is mediated by proteins, such as acid-sensing ion channels (ASICs), membrane-bound receptors whose activation by decreased extracellular pH opens an intrinsic membrane-spanning sodium channel. Curiously, ASICs had only been reported in vertebrates, despite the homology of many other ion channels in vertebrates and invertebrates. Using molecular phylogenetics and electrophysiological recordings, we discover ASICs from tunicates, lancelets, sea urchins, starfish, and acorn worms. This shows that ASICs evolved much earlier than previously thought and suggests that their role in the nervous system is conserved across numerous animal phyla.

Author contributions: T.L., Y.M., J.C.G., and S.A.P. designed research; T.L., Y.M., and J.M.C. performed research; J.M.C. contributed new reagents/analytic tools; T.L., Y.M., J.C.G., and S.A.P. analyzed data; and T.L., Y.M., J.C.G., and S.A.P. wrote the paper.

The authors declare no conflict of interest.

This article is a PNAS Direct Submission.

Data deposition: The sequence reported in this paper has been deposited in the Dryad Digital Data repository, doi: 10.5061/dryad.46320g1.

[1]To whom correspondence should be addressed. Email: tplynagh@gmail.com.

This article contains supporting information online at www.pnas.org/lookup/suppl/doi:10.1073/pnas.1806614115/-/DCSupplemental.

Published online July 30, 2018.

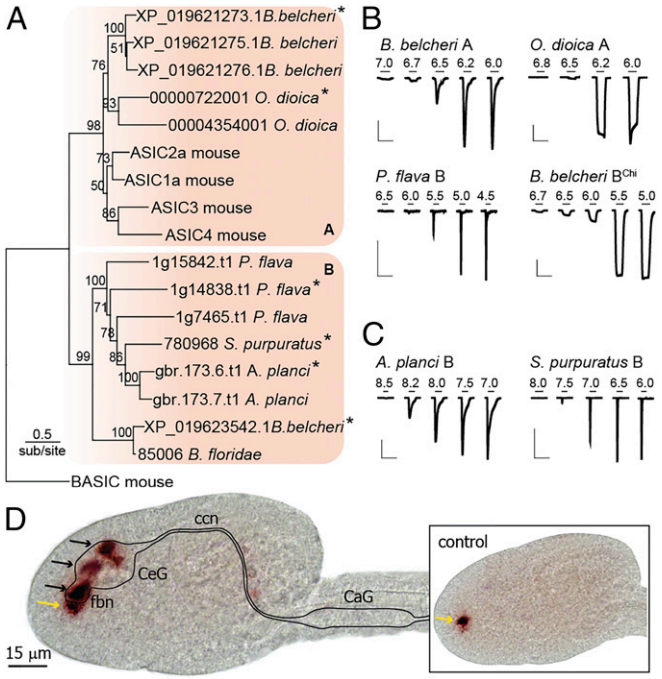

Fig. 1. Deuterostome ASICs identified through phylogenetic and functional analyses. (*A*) Maximum-likelihood tree inferred from alignment of 17 ASIC-like subunits from one vertebrate, one tunicate, two cephalochordates, one hemichordate, and two echinoderms, rooted to mouse BASIC. (*B* and *C*) pH-gated currents in oocytes expressing indicated cRNAs. Resting pH 7.5 (*B*) or 9.0 (*C*). [Scale bars: *x* 20 s; *y* 0.1 μA (*B. belcheri A* and *P. flava B*) or 3 μA (all others).] *B. belcheri* B^{Chi} is a chimera (*SI Appendix, Supplementary Text*). (*D*) In situ hybridization targeting *O. dioica* group A ASIC (black arrows). Illustrated CNS landmarks: CaG, caudal ganglion; ccn, cerebrocaudal nerve; CeG, cerebral ganglion; fbn, first brain nerve. (*Inset*) Control experiment using complementary sense probe showing nonspecific staining in the pharynx (yellow arrows in both sense and antisense experiments).

deuterostomes, protostomes, and xenacoelomorphs comprise the Bilateria, one of the five major lineages of animals [the others being Cnidaria (e.g., hydra), Placazoa, Ctenophora (comb jellies), and Porifera (sponges)]. Previous investigation of ASIC evolution was limited by a vertebrate-centric literature, although an ASIC-like protein from the tunicate *C. intestinalis* was recombinantly expressed, yielding no proton-gated currents (9). To date, proton-activated currents have not been observed in protostome DEG/ENaC channels. To address the occurrence of ASICs in close relatives of the vertebrates, we assembled DEG/ENaC amino acid sequences from one vertebrate, one tunicate, two cephalochordates (both *Branchiostoma* spp.), two echinoderms, and two hemichordates, and assessed the phylogenetic relationship of 102 nonredundant sequences with maximum-likelihood methods (*SI Appendix*, Fig. S1 *A* and *B*). In the resulting tree, several basal branches were poorly supported in bootstrap resampling, but several well-supported clades were identified that include vertebrate channel subunits of established functional properties. One of these clades includes the vertebrate bile acid-sensing ion channel (BASIC), which is not activated by protons (25); another includes vertebrate ENaCs, which are constitutively active (16); and another includes vertebrate ASICs (*SI Appendix*, Fig. S1*A*). The ASIC clade includes sequences from each lineage investigated, suggesting that ASICs could be conserved throughout the deuterostomes.

A maximum-likelihood tree of the deuterostome ASIC-like sequences, rooted to the outgroup of vertebrate BASIC, is shown in Fig. 1*A*, recapitulating the relationships of the overarching tree in *SI Appendix*, Fig. S1, including two well-supported clades within the ASICs (hereafter "group A" and "group B"). Proton-gated currents through channels formed by these subunits would confirm the conservation of ASICs throughout deuterostomes. We therefore synthesized cDNAs (de novo) of at least one subunit from each species addressed (asterisks in Fig. 1*A*), injected cRNAs into *Xenopus* oocytes, and measured current in response to decreased pH. For most channels, rapid application of acidic pH from a resting pH of 7.5 yielded robust proton-gated currents (Fig. 1*B* and Table 1). *Acanthaster planci* and *Strongylocentrotus purpuratus* group B ASICs showed constitutive and no proton-gated current, respectively, with a resting pH of 7.5, but when a resting pH of 9.0 was used, both channels were robustly activated by lower pH (Fig. 1*C* and Table 1). These experiments confirm that ASICs are conserved in each deuterostome lineage, suggesting that ASICs evolved or were already present in ancestral deuterostomes. Phylogenetic analysis including mollusk and arthropod DEG/ENaC sequences returned the very same clade of deuterostome-specific ASIC sequences (*SI Appendix*, Fig. S1*E*), suggesting that ASICs emerged after the protostome/deuterostome split.

Most DEG/ENaC channels selectively conduct sodium ions, with relative permeability over potassium (P_{Na+}/P_{K+}) ranging from ~10 to over 100 (26). We measured P_{Na+}/P_{K+} for newly identified ASICs (*SI Appendix*, Fig. S2*A*) and found that group A ASICs from *Oikopleura dioica* and *Branchiostoma belcheri* showed similar ion selectivity to mouse ASIC1a (also from group A) (Table 1). Surprisingly, group B ASICs showed relatively weak ion selectivity, with P_{Na+}/P_{K+} values closer to unity (Table 1). Because a highly conserved glutamate residue in the channel pore determines ion selectivity in mouse ASIC1a (27), the presence of a neutral glutamine residue at the equivalent position in *Ptychodera flava* and *S. purpuratus* group B ASICs could underlie low selectivity in those channels (*SI Appendix*, Fig. S2*B*). The basis for low selectivity in *B. belcheri* and *A. planci* group B channels is unclear, however, as both possess this glutamate residue, although the *A. planci* channel lacks an aspartate residue near the top of the channel pore that contributes to ion conduction in human ASIC1a (28) (*SI Appendix*, Fig. S2*B*). Nonselective cation current through ASICs is still likely to be excitatory (29), and these results are therefore consistent with a role for ASICs in excitatory signaling throughout deuterostome animals.

If ASICs mediate excitatory neuronal signals in invertebrate deuterostomes, one might expect to find them in the central nervous system (CNS), as is largely the case in rodents and humans (30). To test this, we performed in situ hybridization on the tunicate *O. dioica*, using two antisense probes of different lengths against the *O. dioica* group A ASIC described above. The pattern of ASIC transcript signal was the same for both probes, but varied at different developmental stages. Here we report the temporally most consistent signal, which was localized to the cerebral ganglion, the main hub of the *O. dioica* CNS and the first brain nerves, which convey sensory information from the mouth region (Fig. 1*D*) (31). Control experiments using a complementary sense probe did not yield this signal, but rather nonspecific staining within the pharynx (Fig. 1*D*, control). The CNS localization of an invertebrate ASIC transcript provides additional support for the notion that ASICs contribute to neuronal signaling in invertebrate deuterostomes.

Table 1. Characteristics of deuterostome ASICs (mean ± SD)

	Proton sensitivity			Permeability	
Deuterosome	pH_{50}	n_H	*n*	P_{Na+}/P_{K+}	*n*
Mouse ASIC1a	6.8 ± 0.06	7.6 ± 4.4	6	8.7 ± 1.0	5
O. doica A	6.3 ± 0.02	9.9 ± 0.8	5	10.4 ± 1.9	6
B. belcheri A	6.5 ± 0.04	4.9 ± 1.2	5	12.2 ± 2.7	4
B. belcheri B	5.8 ± 0.03	4.5 ± 0.9	6	1.7 ± 0.2	5
P. flava B	5.5 ± 0.08	2.5 ± 0.9	6	1.9 ± 0.9	6
S. purpuratus B	7.0 ± 0.09	2.4 ± 0.5	5	1.6 ± 0.3	5
A. planci B	8.1 ± 0.05	5.1 ± 2.0	6	3.1 ± 0.4	5

NEUROSCIENCE

A Broader ASIC Comparison Establishes Crucial Determinants of Proton Sensitivity. To distinguish between conserved, fundamental determinants of proton sensing and lineage-specific features, we compared the effects of mutating candidate proton sensors in two distantly related ASICs, mouse ASIC1a (group A) and *B. belcheri* group B^{Chi} (Fig. 1*A*). We focused on four extracellular positions that have emerged as potential proton sensors in structural and functional ASIC studies (18–21), including residues from the β1 strand (H73 in mouse ASIC1a), the β5/β6 loop (K211), the β6/β7 loop (E238), and the α5 helix (D345) (Fig. 2*A* and *SI Appendix*, Fig. S3*A*). The latter two both contribute to the "acidic pocket" that contains several acidic side chains (18). We measured proton sensitivity in mutants where residues were either deleted or substituted (Fig. 2 *B* and *C* and *SI Appendix*, Fig. S3*B*), as it is arguable whether typical charge-neutralizing substitutions, such as D345N, impair (32) or mimic (22) protonation.

Both approaches identified H73 as a crucial determinant of proton sensitivity in distantly related ASICs. In both mouse ASIC1a and in *B. belcheri* group B^{Chi}, the deletion of acidic pocket residues caused significant but relatively moderate decreases in proton sensitivity, whereas the β5/β6 lysine and, especially, the β1 histidine deletions were severely detrimental to proton-gated currents (Fig. 2 *B* and *C* and *SI Appendix*, Fig. S3*A*). In mouse ASIC1a, even the ΔE235-E238 deletion, removing most of this loop from the finger domain in the acidic pocket, did not decrease potency to the extent of ΔH73 or ΔK211 deletions (*SI Appendix*, Fig. S3*A*). The amino acid substitutions revealed a similar pattern, where β1 histidine mutations were by far the most detrimental (*SI Appendix*, Fig. S3*B*). Combined with the high conservation of this residue uniquely in ASICs and the lesser conservation of the β5/β6 lysine and acidic pocket residues, this suggests that the appearance of the histidine residue could underlie the emergence of proton-gated currents (*SI Appendix*, Fig. S3 *C* and *D*).

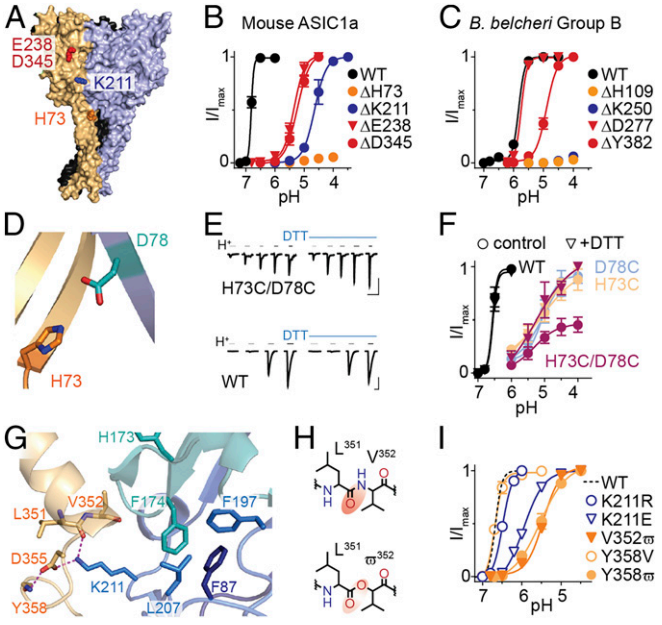

Fig. 2. Determinants of proton sensitivity in broadly related ASICs. (*A*) Chicken ASIC1 structure (PDB ID code 2QTS), different subunits colored orange, blue, and black. Selected side chains are shown in red (acidic pocket), blue (β5/β6 loop from adjacent subunit), and orange (β1 strand). All numbers in this figure refer to equivalent residues in mouse ASIC1a. (*B* and *C*) Normalized peak current responses to decreasing pH for mouse ASIC1a or *B. belcheri* group B^{Chi} ASIC mutants carrying indicated deletions (mean ± SEM, n = 5–7). (*D*) Magnified view of *A* showing H73 and D78 from adjacent subunits. (*E*) Example current responses to acidic pH (gray/black bars) from resting pH of 7.5, alone or with 2 mM DTT. pH for H73C/D87C 6.0/5.5/5.0/4.5/4.0; WT 7.0/6.8/6.5/6.0. [Scale bars: x 20 s; y 100 nA (H73C/D78C) and 3 μA (WT).] (*F*) Normalized responses to acidic pH with/without 2 mM DTT for WT and indicated mouse ASIC1a mutants (mean ± SEM, n = 4). (*G*) Magnified view of *A* showing K211 and selected vicinal side-chain/main-chain atoms. Dashed lines: distance = 2.9 Å. (*H*) Valine (V) and 2-hydroxy-3-methylbutanoic acid (ϖ), red ellipse highlighting decreased electron density. (*I*) Normalized responses to acidic pH for regular substitutions and noncanonical substitutions (mean ± SEM, n = 5–7).

These results suggest intimate roles for the β1 strand and the β5/β6 loop in ASIC activation. Because recent structural and earlier mutagenesis studies implicate β1/β1 rearrangements in activation by protons (20, 33), we substituted H73 and D78 residues for cysteine in mouse ASIC1a and looked for changes in proton-gated currents in the presence of the reducing agent DTT, which would be indicative of a disulfide cross-link between adjacent β1 domains (34). As expected, activation of mutant H73C/D78C channels required much higher proton concentrations than WT channels (Fig. 2 *E* and *F*). In the presence of DTT, peak current amplitude was approximately doubled in H73C/D78C channels (and not in WT or single-mutant H73C or D78C channels), suggesting that a link between introduced cysteine residues forms spontaneously and is broken upon reduction. There was no significant difference in pH_{50} without (5.1 ± 0.1, n = 4) and with DTT (5.0 ± 0.4, n = 4; P = 0.959), suggesting that the β1-β1 cross-link causes smaller currents by precluding activation of many channels, rather than shifting the gating equilibrium of all channels. We also observed that application of DTT immediately preceding acidic pH increased current amplitudes, whereas coapplication of DTT during acidic pH had no effect on current amplitude (*SI Appendix*, Fig. S4*A*). These results confirm that β1/β1 interactions affect channel activation by protons and suggest that enforced 73/78 proximity in resting channels stabilizes a state from which activation proceeds poorly.

Structural data place the K211 side-chain nitrogen atom <3 Å from both the main chain carbonyl oxygen of L351 and the side chain carboxylate of D355 (Fig. 2*G*), and D355 mutations were previously shown to impair ASIC1a activation (20, 21). Here we questioned the role of a potential hydrogen bond (H bond) between K211 and L351 by replacing V352 with 2-hydroxy-3-methylbutanoic acid (ϖ). This withdraws electron density from the backbone carbonyl oxygen of L351 (Fig. 2*H*), making the latter a weaker H-bond acceptor (27). V352ϖ channels showed substantially reduced proton sensitivity compared with WT (Fig. 2*I* and *SI Appendix*, Fig. S4*C*) (pH_{50} = 5.47 ± 0.05, n = 7, P < 0.001 compare with WT), providing evidence that a K211/L351 H bond is important for ASIC1a activation. This is supported by our observation that the K211R substitution, retaining a strong H-bond donor, is well tolerated compared with the K211E substitution, which removes a strong H-bond donor (Fig. 2*I*). Another potential H bond in this domain appears between the carboxylate side chain of D355 and the main-chain nitrogen of Y358 (Fig. 2*G*), which we probed by measuring proton sensitivity of Y358ϖ channels, in which the main-chain H-bond donor (NH) is replaced by an acceptor (CO). The Y358ϖ substitution (pH_{50} = 5.51 ± 0.14, n = 7, P < 0.001 compared with WT) caused a similar decrease in proton sensitivity as the V352ϖ substitution, whereas the Y358V substitution did not differ from WT (Fig. 2*I* and *SI Appendix*, Fig. S4*C*). This provides evidence for an additional H bond in this domain contributing to proton sensitivity, and we conclude that in ASIC1a, K211 bridges thumb and palm domains of adjacent subunits via an H-bond network.

Unlike several other loops in the ASIC extracellular domain, the β5/β6 loop containing K211 is not stabilized by endogenous disulfides. We therefore questioned how K211 rearrangements could be stably coupled to conformational changes "downstream," toward the channel domain. We noticed that two hydrophobic side chains of the β5/β6 loop interact closely with hydrophobic side chains from the β3/β4 and β1/β2 loops of the same subunit in crystal structures (Fig. 2*G* and *SI Appendix*, Fig. S5*A*). Hypothesizing that these interactions couple β5/β6 activity to channel activity, we tested the role of these large hydrophobic side chains by substituting them with alanine and recording

proton-gated currents in mouse ASIC1a. β3/β4 F174A, β5/β6 F197A, and L207A, and especially β1/β2 F87A substitutions substantially reduced proton sensitivity compared with WT (*SI Appendix*, Fig. S5 *B* and *C*). Notably, the H173A mutation, adjacent to F174 but oriented away from this hub, had no effect on proton sensitivity (*SI Appendix*, Fig. S5). This suggests that a hub of hydrophobic side chains may provide a stable link between two crucial domains: the interface of adjacent β1 strands and the more extracellular interface of thumb (α5) and palm (β5/β6 loop) domains.

Loss of Proton Sensitivity in ASIC4 in Mammals. We next questioned why rat ASIC4 is apparently insensitive to protons, despite proton-gated currents in zebrafish ASIC4.1 and evidence for ASIC4 transcripts in the rat brain (35–37). Assessing the phylogenetic relationship of ASIC4 sequences showed broad conservation of ASIC4 throughout the vertebrates, with a maximum-likelihood tree of vertebrate ASIC4 sequences generally reflecting the overarching evolution of vertebrate animals (Fig. 3*A*). To establish where in the vertebrate lineage proton sensitivity of ASIC4 was lost, we tested ASIC4 channels from three major lineages between bony fishes and mammals: coelacanth (lobe-finned fish), frog, and chicken. Each of these ASICs showed proton-gated currents, although current amplitude was small and variable (Fig. 3). We therefore tested a mutated version of each channel, carrying a 24-amino acid deletion in the N terminal (hereafter "Δ24"), which has been shown to enhance zebrafish ASIC4 expression (38). Coelacanth, frog, and chicken ASIC4$^{\Delta 24}$ channels showed larger currents in response to acidic pH, whereas rat ASIC4$^{\Delta 24}$ remained unresponsive (Fig. 3). Thus, as ASIC4 in all vertebrate lineages except mammalian shows some proton-gated current, we conclude that ASIC4 was proton-sensitive in the ancestor of reptilian and mammalian lineages and lost proton sensitivity in the latter.

We aligned rat ASIC4 with proton-sensitive ASIC sequences, looking for amino acid sequence differences that might underlie the loss of proton sensitivity, but crucial residues were largely conserved, including β1 H73 and D78 and β1/β2 F87 (*SI Appendix*, Fig. S6*A*). We therefore turned to a different approach and generated chimeric channels based on proton-insensitive rat ASIC4$^{\Delta 24}$ and containing one to three segments of highly proton-sensitive mouse ASIC1a sequence (Fig. 4*A* and *SI Appendix*, Fig. S6*A*). Segment 1 (25 residues) consisted primarily of the β1 strand containing H73/D78 and was chosen based on our results (Fig. 2) and on previous work showing that this segment is crucial for proton-gated currents (10, 38). Segment 2 (17 residues) included parts of β3/β4 and β5/β6

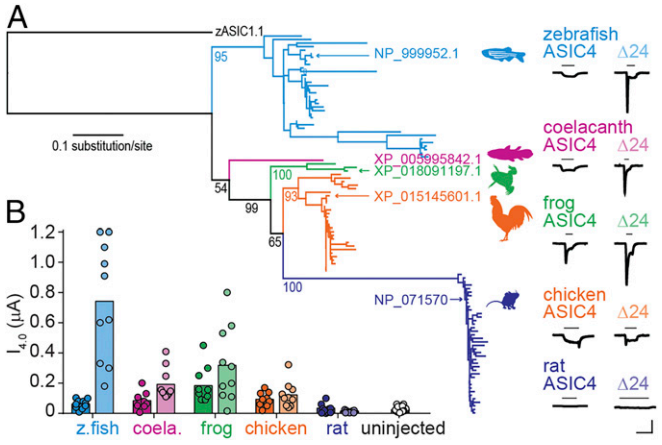

Fig. 3. Proton sensitivity in vertebrate ASIC4. (*A*) Maximum-likelihood tree of ASIC4 amino acid sequences, rooted to zebrafish ASIC1.1. Bootstrap support (per 100) shown for selected branches. Example pH 4.0-gated currents for indicated ASICs shown on right. (Scale bars: *x* 10 s; *y* 0.1 μA.) "Δ24" constructs lack 24 N-terminal amino acids following the starting methionine. (*B*) Average (column) and individual (dots) pH 4.0-gated peak current amplitudes (color as in *A*). *n* = 10, except for uninjected, *n* = 25.

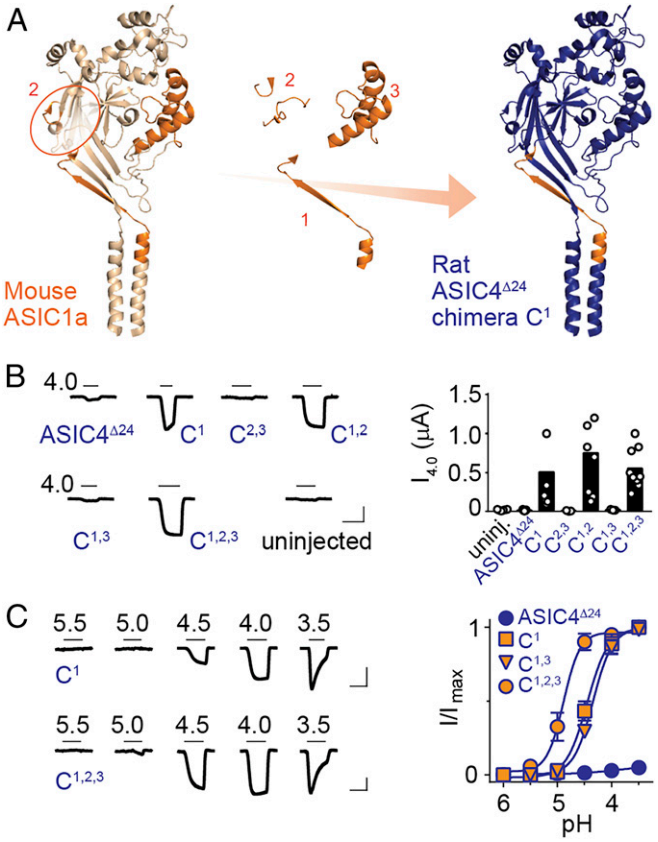

Fig. 4. ASIC1a β1 segment confers proton sensitivity on ASIC4. (*A*) Cartoon illustrating ASIC1a segments that were substituted into ASIC4 (segment 2 circled for clarity). (*B*) Example currents (*Left*) and mean peak current amplitude (black columns, *Right*) in response to pH 4.0 at indicated constructs. (*C*) Example currents (*Left*) and mean (±SEM, *n* = 5–6), normalized responses (*Right*) to decreasing pH. (Scale bars in *B* and *C*: *x* 5 s, *y* 0.1 μA.)

(including K211) loops, and segment 3 (54 residues) consisted primarily of the thumb domain α4 and α5 helices. These were chosen based on findings that interfacial interactions between thumb and β3/β4 and β5/β6 loops contribute to proton sensitivity (Fig. 2) (20, 39). We hypothesized that alone, segment 1 of ASIC1a might confer proton-gated currents on rat ASIC4$^{\Delta 24}$ and the additional combination of segments 2 and 3 might render rat ASIC4$^{\Delta 24}$ more sensitive to protons by introducing more favorable interactions between adjacent subunits.

Remarkably, chimera C^1, containing only segment 1 from mouse ASIC1a, showed robust proton-gated currents, with a pH_{50} of 4.5 ± 0.2 (*n* = 6) (Fig. 4 *B* and *C*), confirming that this segment is crucial for proton-gated currents. In contrast, chimera C^{2,3}, containing only segments 2 and 3 and thus a putative ASIC1a-like intersubunit interface around K211, showed no responses to pH 4 (Fig. 4*B*). Combining either segment 2 or 3 with segment 1 (in chimeras C^{1,2} and C^{1,3}) had no effect on proton sensitivity relative to chimera C^1 or abolished proton-gated currents, respectively (Fig. 4 *B* and *C*). However, adding both extracellular segments to chimera C^1, yielding chimera C^{1,2,3}, caused a significant increase in proton sensitivity relative to chimera C^1 (Fig. 4*C*), reflected in the higher pH_{50} value of 4.9 ± 0.2 for chimera C^{1,2,3} (*n* = 6, *P* = 0.001). Thus, the ASIC1a β1 segment renders ASIC4 a proton-gated channel, and adding ASIC1a-like thumb domain/palm domain interfaces increases proton sensitivity. Considering which β1 amino acid differences make mammal ASIC4 proton-insensitive, we noticed an insertion in mammal ASIC4 preceding the conserved β1/β2 phenylalanine residue (*SI Appendix*, Fig. S6*A*). Inserting this residue into proton-sensitive chimera C^1 (rat ASIC4$^{\Delta 24}$ with ASIC1a

NEUROSCIENCE

β1) abolished proton-gated currents (*SI Appendix*, Fig. S6*B*), suggesting that such a mutation could have contributed to the loss of proton sensitivity in mammal ASIC4. Deleting the equivalent residue from ASIC4 β1 failed to confer proton-gated currents on rat ASIC4$^{\Delta 24}$, unlike replacing the entire ASIC4 β1 with that of ASIC1a (*SI Appendix*, Fig. S6*B*). Taken together, these results suggest that proton insensitivity in mammal ASIC4 is due to several differences from other ASICs in the β1 segment, including a different number of residues in this segment, and that low proton sensitivity in ASIC4 also derives from divergence in the intersubunit interface around K211.

Discussion

Gain of Proton Sensing and Potential Roles for ASICs in Invertebrate Neurophysiology. Previous work identified ASIC subunits from the tunicate *C. intestinalis*, the jawless fish *L. fluviatilis*, and the cartilaginous fish *Squalus acanthias*, which formed membrane proteins that were not activated by protons (9, 10). With 34–66% identity with rat ASIC1a, these sequences certainly fit into the ASIC clade we now describe, but their proton insensitivity and the absence of data on other deuterostome ASICs at the time led to the logical conclusion that DEG/ENaC sequences developed proton-gated currents after the bony fishes split from the cartilaginous fishes (10), ∼420 Mya, well after chordates split from other deuterostomes (40). We sampled recent genetic data from a broad selection of deuterostome animals, to assess the phylogenetic relationships of ASIC sequences and measure the function of recombinantly expressed channels. Our phylogenetic and functional analyses identify ASICs from each deuterostome lineage that form a well-supported clade within the overarching DEG/ENaC family. Within the ASIC clade are two well-supported groups, and although ASICs of vertebrates and tunicates appear in only group A and ASICs of echinoderms and hemichordates appear only in group B, there is good support for cephalochordate ASICs in both clades (*SI Appendix*, Fig. S1*C*). This suggests that an ancestral chordate possessed genes from both groups, and group B ASICs were lost in Olfactores (tunicates + vertebrates), although this tentative hypothesis would benefit from broader sampling in future. In any case, the presence of ASICs in ancestral deuterostomes means that ASICs emerged at least 600 Mya, well before the Cambrian explosion (41). Tentative phylogenetic evidence suggests that ASICs evolved after the protostome/deuterostome split.

We find that in the tunicate *O. dioica*, transcripts of a functional ASIC are consistently found within the cerebral ganglion, a structure that is homologous to the vertebrate brain, integrates input from a variety of sensory nerves, and dynamically regulates more caudal CNS structures (42–44). This CNS localization accords with several roles for ASICs in the vertebrate CNS, including stress responses (45) and synaptic plasticity at central glutamatergic synapses (6, 7). Because protons are coreleased with glutamate (46), and glutamatergic signaling underlies synaptic plasticity in both deuterostomes and protostomes (4, 5), we suggest that ASICs could also contribute to synaptic plasticity in invertebrates.

Loss of Proton Sensing in ASIC4. Vertebrates possess four ASIC genes, the products of which form homo- or hetero-trimeric channels of varying proton sensitivity and expression patterns (26). Vertebrate ASIC4 is curious in that transcripts are expressed in various loci of human, rat, mouse, and rabbit brain (30), yet when expressed recombinantly it does not form functional channels, despite cell surface localization (35, 47, 48). Certain studies suggest that ASIC4 may coassemble with other ASIC subunits and reduce their function through intracellular compartmentalization or degradation (47, 49). We report proton-gated currents through ASIC4 channels from fish, frog, and chicken and find that this property was completely lost in the mammalian lineage. It is conceivable that coassembly/internalization functions of ASIC4 evolved before it lost proton sensitivity, such that proton sensitivity became redundant in mammal ASIC4 and numerous substitutions detrimental to proton sensitivity could then accumulate. Nonetheless, our results with ASIC1a/ASIC4 chimeras and ASIC4 mutants indicate that inactivity of mammal ASIC4 is determined by a 24-amino acid segment just external to the channel domain, which includes a functionally detrimental single amino acid insertion. Certain other ASICs also appear to have lost proton sensitivity, including one from *C. intestinalis* (9) and another from *O. dioica* (*SI Appendix*, Fig. S1*A*), which contains a similar amino acid insertion as mammal ASIC4 (*SI Appendix*, Fig. S6*C*).

Molecular Determinants of Proton Sensitivity. Our experiments with diverse proton-sensitive ASICs reiterate the key role of the β1 segment, in particular a histidine residue conserved in all ASICs we characterized, suggesting it was present in the ancestral deuterosome ASIC. Furthermore, we show that linking adjacent β1 strands in resting channels precludes channel activation. This is reflected in the dynamic role of β1 emerging from the assessment of resting and open-state chicken ASIC1 X-ray structures, where the base of β1 appears to move away from that of adjacent β1 strands, pulling the channel open (33). Others proposed that protonation of H73 facilitates a H73/D78 interaction (20), although H73/D78 Cα/Cα distances differ little in resting and open structures (9.3 Å in PDB ID code 5WKU; compare with 10.1 Å in PDB ID code 4NTW). However, the resting-state C73/C78 cross-link formed spontaneously, despite ∼6.3-Å separation of these sulfhydryls in 5WKU (as measured by H73/D78 Cγ atoms), implying flexibility in this domain even at rest.

H73 could, together with D78, act as both a proton sensor and part of a transduction pathway between more external proton sensors and the channel domain. Its position seems suited to this and is similar to that of key proton sensors in proton-gated channels from other protein families (50). Because H73 is conserved throughout the extended ASIC family (*SI Appendix*, Fig. S3*C*), it was likely present in the earliest deuterostome ASIC, and we speculate that it was the key to the evolution of proton-gated currents. We suppose that over time—before and after the emergence of proton-gated currents—ASICs have undergone other lineage-specific mutations that alter proton sensitivity. Such elaborations may be sufficient for activation even in the absence of H73 [e.g., in zebrafish ASIC1.1 (37)] and may include K211 and the acidic pocket, which is poorly developed in group B ASICs but more extensive in group A ASICs, such as vertebrate ASIC1a (18) (*SI Appendix*, Fig. S3*C*).

K211 contributes to proton sensitivity by bridging palm and thumb domains of adjacent subunits, consistent with a decrease in K211 Cα/L351 CO distance of 1.3 Å from resting to open channel structures (33, 51). Whether K211 is uncharged at neutral pH and is protonated by low pH remains unclear, but we note that pK_a values for buried lysine side chains, especially in close proximity to carboxylate or carbonyl atoms, can be lower than 6.0 (52). Tentative support for the notion that K211 is uncharged in resting and charged in activated/desensitized channels comes from the absence of negatively charged chloride ions near K211 in the pH ∼ 8.0 resting-state structure (33) and close proximity of chloride ions to the K211 amine in pH 5.0–6.0 structures (18, 51). We identify a hydrophobic hub ideally poised to couple motions around β5/β6 K211 to those around β1 H73. In line with this hypothesis, in the hydrophobic hub, the Cα/Cα distance between β5/β6 L207 and β1/β2 F87 remains 5.5 Å in both the resting- and open-state structures, in contrast to the β5/β6 and β1 domains themselves, which undergo more noticeable rearrangements.

Summary. This work shifts the estimate of the origin of ASICs from after to before the Cambrian explosion, and it shows that the loss of proton sensitivity in ASIC4 occurred after vertebrates moved onto land. The occurrence of ASICs in invertebrates points toward additional homology between invertebrate and vertebrate nervous systems regarding excitatory neurotransmission.

Methods

ASICs were identified by alignment and phylogenetics of 102 DEG/ENaC amino acid sequences from deuterostomes. One sequence from each lineage (asterisks in Fig. 1*A*) was selected for commercial cDNA synthesis, cRNAs were injected into *Xenopus laevis* oocytes, and proton-gated currents were measured with two-electrode voltage clamp (TEVC). Whole-mount in situ hybridization (53) used 8-h postfertilization *O. dioica* and RNA probes targeting group A ASIC from *O. dioica*. Mouse ASIC1a and *B. belcheri* group B ASIC mutants (Fig. 2) were generated with site-directed mutagenesis and tested with TEVC. We used 108 vertebrate ASIC4 sequences to establish phylogenetic relationships of ASIC4 (Fig. 3). Three were selected for cDNA synthesis and TEVC, as were chimeric constructs from Fig. 4. See *SI Appendix, Supplementary Text* for detailed description of materials and methods.

ACKNOWLEDGMENTS. This work was funded by the Danish Council for Independent Research (T.L.), the Lundbeck Foundation (T.L. and S.A.P.), the Carlsberg Foundation (S.A.P.), the Novo Nordisk Foundation (S.A.P.), and the Norwegian Research Council (J.C.G.).

1. Smart TG, Paoletti P (2012) Synaptic neurotransmitter-gated receptors. *Cold Spring Harb Perspect Biol* 4:a009662.
2. Liebeskind BJ, Hillis DM, Zakon HH (2015) Convergence of ion channel genome content in early animal evolution. *Proc Natl Acad Sci USA* 112:E846–E851.
3. Moroz LL, et al. (2014) The ctenophore genome and the evolutionary origins of neural systems. *Nature* 510:109–114.
4. Dale N, Kandel ER (1993) L-glutamate may be the fast excitatory transmitter of Aplysia sensory neurons. *Proc Natl Acad Sci USA* 90:7163–7167.
5. Nicoll RA (2017) A brief history of long-term potentiation. *Neuron* 93:281–290.
6. Du J, et al. (2014) Protons are a neurotransmitter that regulates synaptic plasticity in the lateral amygdala. *Proc Natl Acad Sci USA* 111:8961–8966.
7. Kreple CJ, et al. (2014) Acid-sensing ion channels contribute to synaptic transmission and inhibit cocaine-evoked plasticity. *Nat Neurosci* 17:1083–1091.
8. Wemmie JA, Taugher RJ, Kreple CJ (2013) Acid-sensing ion channels in pain and disease. *Nat Rev Neurosci* 14:461–471.
9. Coric T, Passamaneck YJ, Zhang P, Di Gregorio A, Canessa CM (2008) Simple chordates exhibit a proton-independent function of acid-sensing ion channels. *FASEB J* 22: 1914–1923.
10. Coric T, Zheng D, Gerstein M, Canessa CM (2005) Proton sensitivity of ASIC1 appeared with the rise of fishes by changes of residues in the region that follows TM1 in the ectodomain of the channel. *J Physiol* 568:725–735.
11. Dymowska AK, Schultz AG, Blair SD, Chamot D, Goss GG (2014) Acid-sensing ion channels are involved in epithelial Na+ uptake in the rainbow trout *Oncorhynchus mykiss*. *Am J Physiol Cell Physiol* 307:C255–C265.
12. Price MP, et al. (2001) The DRASIC cation channel contributes to the detection of cutaneous touch and acid stimuli in mice. *Neuron* 32:1071–1083.
13. Hill A, et al. (2017) The *Drosophila* postsynaptic DEG/ENaC channel *ppk29* contributes to excitatory neurotransmission. *J Neurosci* 37:3171–3180.
14. Goodman MB, et al. (2002) MEC-2 regulates *C. elegans* DEG/ENaC channels needed for mechanosensation. *Nature* 415:1039–1042.
15. Golubovic A, et al. (2007) A peptide-gated ion channel from the freshwater polyp Hydra. *J Biol Chem* 282:35098–35103.
16. Lingueglia E, Champigny G, Lazdunski M, Barbry P (1995) Cloning of the amiloride-sensitive FMRFamide peptide-gated sodium channel. *Nature* 378:730–733.
17. Canessa CM, Horisberger JD, Rossier BC (1993) Epithelial sodium channel related to proteins involved in neurodegeneration. *Nature* 361:467–470.
18. Jasti J, Furukawa H, Gonzales EB, Gouaux E (2007) Structure of acid-sensing ion channel 1 at 1.9 A resolution and low pH. *Nature* 449:316–323.
19. Li T, Yang Y, Canessa CM (2009) Interaction of the aromatics Tyr-72/Trp-288 in the interface of the extracellular and transmembrane domains is essential for proton gating of acid-sensing ion channels. *J Biol Chem* 284:4689–4694.
20. Paukert M, Chen X, Polleichtner G, Schindelin H, Gründer S (2008) Candidate amino acids involved in H+ gating of acid-sensing ion channel 1a. *J Biol Chem* 283:572–581.
21. Sherwood T, et al. (2009) Identification of protein domains that control proton and calcium sensitivity of ASIC1a. *J Biol Chem* 284:27899–27907.
22. Vullo S, et al. (2017) Conformational dynamics and role of the acidic pocket in ASIC pH-dependent gating. *Proc Natl Acad Sci USA* 114:3768–3773.
23. Delsuc F, Brinkmann H, Chourrout D, Philippe H (2006) Tunicates and not cephalochordates are the closest living relatives of vertebrates. *Nature* 439:965–968.
24. Cannon JT, et al. (2016) Xenacoelomorpha is the sister group to Nephrozoa. *Nature* 530:89–93.
25. Wiemuth D, Assmann M, Gründer S (2014) The bile acid-sensitive ion channel (BASIC), the ignored cousin of ASICs and ENaC. *Channels (Austin)* 8:29–34.
26. Kellenberger S, Schild L (2015) International Union of Basic and Clinical Pharmacology. XCI. Structure, function, and pharmacology of acid-sensing ion channels and the epithelial Na+ channel. *Pharmacol Rev* 67:1–35.
27. Lynagh T, et al. (2017) A selectivity filter at the intracellular end of the acid-sensing ion channel pore. *eLife* 6:e24630.
28. Yang L, Palmer LG (2014) Ion conduction and selectivity in acid-sensing ion channel 1. *J Gen Physiol* 144:245–255.
29. Wollmuth LP (2018) Ion permeation in ionotropic glutamate receptors: Still dynamic after all these years. *Curr Opin Physiol* 2:36–41.
30. Deval E, Lingueglia E (2015) Acid-sensing ion channels and nociception in the peripheral and central nervous systems. *Neuropharmacology* 94:49–57.
31. Søviknes AM, Glover JC (2007) Spatiotemporal patterns of neurogenesis in the appendicularian *Oikopleura dioica*. *Dev Biol* 311:264–275.
32. Yang H, et al. (2009) Inherent dynamics of the acid-sensing ion channel 1 correlates with the gating mechanism. *PLoS Biol* 7:e1000151.
33. Yoder N, Yoshioka C, Gouaux E (2018) Gating mechanisms of acid-sensing ion channels. *Nature* 555:397–401.
34. Akabas MH (2015) Cysteine modification: Probing channel structure, function and conformational change. *Novel Chemical Tools to Study Ion Channel Biology*, eds Ahern C, Pless S (Springer, New York), pp 25–54.
35. Akopian AN, Chen CC, Ding Y, Cesare P, Wood JN (2000) A new member of the acid-sensing ion channel family. *Neuroreport* 11:2217–2222.
36. Gründer S, Geissler HS, Bässler EL, Ruppersberg JP (2000) A new member of acid-sensing ion channels from pituitary gland. *Neuroreport* 11:1607–1611.
37. Paukert M, et al. (2004) A family of acid-sensing ion channels from the zebrafish: Widespread expression in the central nervous system suggests a conserved role in neuronal communication. *J Biol Chem* 279:18783–18791.
38. Chen X, Polleichtner G, Kadurin I, Gründer S (2007) Zebrafish acid-sensing ion channel (ASIC) 4, characterization of homo- and heteromeric channels, and identification of regions important for activation by H+. *J Biol Chem* 282:30406–30413.
39. Gwiazda K, Bonifacio G, Vullo S, Kellenberger S (2015) Extracellular subunit interactions control transitions between functional states of acid-sensing ion channel 1a. *J Biol Chem* 290:17956–17966.
40. Brazeau MD, Friedman M (2015) The origin and early phylogenetic history of jawed vertebrates. *Nature* 520:490–497.
41. Swalla BJ, Smith AB (2008) Deciphering deuterostome phylogeny: Molecular, morphological and palaeontological perspectives. *Philos Trans R Soc Lond B Biol Sci* 363: 1557–1568.
42. Bollner T, Storm-Mathisen J, Ottersen OP (1991) GABA-like immunoreactivity in the nervous system of *Oikopleura dioica* (Appendicularia). *Biol Bull* 180:119–124.
43. Kreneisz O, Glover JC (2015) Developmental characterization of tail movements in the appendicularian urochordate *Oikopleura dioica*. *Brain Behav Evol* 86:191–209.
44. Søviknes AM, Chourrout D, Glover JC (2005) Development of putative GABAergic neurons in the appendicularian urochordate *Oikopleura dioica*. *J Comp Neurol* 490: 12–28.
45. Coryell MW, et al. (2009) Acid-sensing ion channel-1a in the amygdala, a novel therapeutic target in depression-related behavior. *J Neurosci* 29:5381–5388.
46. Brown JT, et al. (2010) Vesicular release of glutamate utilizes the proton gradient between the vesicle and synaptic cleft. *Front Synaptic Neurosci* 2:15.
47. Donier E, Rugiero F, Jacob C, Wood JN (2008) Regulation of ASIC activity by ASIC4—New insights into ASIC channel function revealed by a yeast two-hybrid assay. *Eur J Neurosci* 28:74–86.
48. Gründer S, Pusch M (2015) Biophysical properties of acid-sensing ion channels (ASICs). *Neuropharmacology* 94:9–18.
49. Schwartz V, Friedrich K, Polleichtner G, Gründer S (2015) Acid-sensing ion channel (ASIC) 4 predominantly localizes to an early endosome-related organelle upon heterologous expression. *Sci Rep* 5:18242.
50. Nemecz Á, et al. (2017) Full mutational mapping of titratable residues helps to identify proton-sensors involved in the control of channel gating in the *Gloeobacter violaceus* pentameric ligand-gated ion channel. *PLoS Biol* 15:e2004470.
51. Baconguis I, Bohlen CJ, Goehring A, Julius D, Gouaux E (2014) X-ray structure of acid-sensing ion channel 1-snake toxin complex reveals open state of a Na(+)-selective channel. *Cell* 156:717–729.
52. Isom DG, Castañeda CA, Cannon BR, García-Moreno B (2011) Large shifts in pKa values of lysine residues buried inside a protein. *Proc Natl Acad Sci USA* 108: 5260–5265.
53. Mikhaleva Y, Kreneisz O, Olsen LC, Glover JC, Chourrout D (2015) Modification of the larval swimming behavior in *Oikopleura dioica,* a chordate with a miniaturized central nervous system by dsRNA injection into fertilized eggs. *J Exp Zool B Mol Dev Evol* 324:114–127.